JOURNAL OF MATERIALS SCIENCE 26 (1991) 925–939

The frictional behaviour of LiF single crystals

E. A. SCHLANGER
265 East 66th Street, No. 44A, New York, New York 10021, USA

C. Y. HUANG
Materials Research Laboratory, The Pennsylvania State University, University Park, Pennsylvania 16802, USA

N. H. MACMILLAN*
Department of Mechanical Engineering, Oregon State University, Corvallis, Oregon 97331, USA

A study has been made of the influence of initial surface roughness, renewable and non-renewable surface contaminants, and irradiation hardening on the coefficient of friction for one LiF single crystal (A) sliding on another (B) in $\{1\,0\,0\}_A\langle 0\,1\,0\rangle_A \parallel \{1\,0\,0\}_B\langle 0\,1\,0\rangle_B$ orientation at $\sim$ 295 K. The normal load was $\sim$ 1 N, the nominal contact pressure $\sim$ 0.1 MPa, the sliding velocity 0.2 to 0.6 mm sec^{-1}, and the amplitude of the (reciprocate) motion a few millimetres. Any influence of non-renewable contaminants persisted only for cumulative relative displacements $\lesssim$ 0.1 m, and that of micrometre-scale initial surface roughness only for a few metres. At steady state in the presence of renewable contaminants the coefficient of friction varied only from a high of $\sim$ 0.45 in ultra-high vacuum ($\sim 7.5 \times 10^{-8}$ Pa) and "dry" nitrogen-rich air ($\sim 10^5$ Pa, relative humidity $\lesssim$ 15%) to a low of $\sim$ 0.38 in "moist" nitrogen-rich air ($\sim 10^5$ Pa, relative humidity $\sim$ 50%). Irradiation hardening had no effect on the coefficient of friction at steady state. The worn surfaces created by steady-state sliding always exhibited a grooved topography partly obscured by more-or-less adherent layers of variously consolidated equiaxed debris particles $\sim$ 100 nm in size. Owing to the action of image forces, these particles contained no dislocations. It is suggested that the coefficient of friction was determined at steady state by the stress needed to shear these tiny particles past one another as near-rigid bodies.

1. Introduction

Current understanding of friction derives from the development, primarily by the Cambridge school led by Bowden and Tabor [1], of ideas due originally to da Vinci [2], Amontons [3], Coulomb [4] and Leslie [5]. The essential concept is that surfaces are normally rough on the atomic scale, and that under typical service conditions they make contact only at the tips of asperities. Now, strong (ionic, covalent or metallic) bonds form between opposing asperities when these close to within $\sim$ 1 nm, and weaker van der Waals bonds form at larger separations. These bonds can transmit loads applied to one body across a contact interface with a second body, thereby creating stresses in both bodies. As these stresses increase they lead first to reversible (elastic) deformation at the points of contact, and thereafter to irreversible deformation. This latter process leads in turn to dissipation of energy, which manifests itself as frictional resistance to interfacial sliding, and to the accumulation of damage, which manifests itself as wear. Once wear debris starts to form in significant quantities, the evolution of the contact depends critically on the size and morphology of the particles produced and on how effectively these particles are trapped at the sliding interface. It is clear that such discrete particles represent a mobile type of asperity very different from the immobile type formed on and contiguous with a bulk substrate. Frictional behaviour in the debris-dominated regime is even less well understood than that in the early stages of running-in.

In the case of a bulk crystal deformed at a temperature less than about half of its (absolute) melting point, the important mechanisms of irreversible deformation normally are dislocation glide and crack propagation. These processes "compete" to lower the free energy of the system "crystal plus applied forces", and the outcome of their competition determines whether the crystal behaves in a ductile or a brittle fashion.

This competition is always interesting in the case of the alkali halides, because its outcome is by no means

* *Present address*: Division of Ceramic Engineering and Science, New York State College of Ceramics at Alfred University, Alfred, New York 14802, USA.

0022–2461/90 $03.00 + .12

certain – the description of such crystals as semi-brittle is apt; and in the case of sliding contact between two such crystals having surface roughnesses typical of modern engineering practice (i.e. 0.1 to 10 μm) the competition becomes doubly interesting. This is partly because deformation occurs during such a contact under multi-axial and dominantly compressive loading, but much more because the linear dimension of the volume stressed at a typical junction between opposing asperities on such surfaces is small compared both with the average spacing between grown-in dislocations (~ 100 μm at a typical density of $10^8\,m^{-2}$ [6]) and with the range of the elastic stress field of a dislocation (a good rule of thumb is that half of the elastic strain energy of an isolated dislocation in a typical laboratory (centimetre)-scale specimen resides more than 1 μm from its core). Grown-in dislocations may thus be expected to play little role in determining the mechanical behaviour of a typical such junction, regardless of their mobility (or lack thereof). More importantly, dislocations created during the contact are likely to interact as strongly with the surface as with other dislocations, i.e. image forces are likely to be as important to the outcome of the competition as dislocation–dislocation interactions. Further, slip flexibility is likely to be restricted in such a small volume [7], and both the nucleation of a new crack and the propagation of either a new or a pre-existing crack become more difficult as the stressed volume decreases [7]. The final interesting feature of the competition is that such a small stressed volume typically lies entirely within the space charge layers formed at the surfaces of the two crystals [8, 9], with the result that its deformation is susceptible to the numerous subtle influences which physisorption and/or chemisorption can exert on dislocation glide and crack propagation [10–12].

For all of the above reasons, there is much uncertainty about the relative contributions of dislocation glide and crack propagation to the friction and wear of the alkali halides (and other more-or-less brittle crystals). Accordingly, an attempt has been made to throw some light on this question. Friction measurements have been made on surfaces of LiF single crystals covered with asperities of different (initial) size both *in vacuo* and in an environment known to influence the near-surface mechanical behaviour of such crystals [13–21]. In addition, the effect of irradiation hardening on friction has been compared with its effects on yield strength and hardness. The rationale for this last part of the work is that such hardening can be expected to have very different effects on the mobilities of primary ($\{1\,1\,0\}\langle 1\,\bar{1}\,0\rangle$) and secondary ($\{1\,0\,0\}\langle 1\,\bar{1}\,0\rangle$) glide dislocations without affecting the adhesion between asperities. Also reported are some transient effects on friction of non-renewable surface contaminants adsorbed during specimen preparation.

2. Experimental procedure

2.1. Materials

All experiments were performed at ambient temperature (~ 295 K) on melt-grown single crystals of LiF supplied by Harshaw Chemical Co., Solon, Ohio. These were gamma-irradiated in uncontrolled fashion prior to shipment to make them harder and easier to cleave, and from their deep yellow colour it was estimated visually that they contained 10^{14} to 10^{15} F centres (and aggregates thereof) per cubic millimetre [22–24]. They were tested both as-received and following annealing in air for 1 h at 750 K to eliminate the radiation damage. All annealed crystals were completely colourless. Etch-pitting studies [25, 26] revealed the grown-in dislocation density to be 10^8 to $10^9\,m^{-2}$, with most of these dislocations forming low-angle boundaries between millimetre-scale subgrains. Finally, emission spectrographic analysis of a solution prepared by dissolving pieces of several crystals in HNO_3 showed that their principal impurities were (in p.p.m.): Si 100, Mg 23, Fe 6, Al 4 and Ca 2. A duplicate analysis carried out using plastic rather than silica glass containers gave almost the same result.

2.2. Methods

Vickers hardness, H_v, was measured on $\{1\,0\,0\}$ cleavage surfaces in air of uncontrolled humidity, using a load of 1 N and a loading time of 10 sec. For such a load and loading time, the influence of environment on H_v should be small [10, 13, 14, 20]. The indentation was always oriented with its diagonals parallel to $\langle 1\,0\,0\rangle$.

The yield strength, σ_y, in uniaxial compression was measured on an Instron universal testing machine at a strain rate of about $2 \times 10^{-4}\,sec^{-1}$. The specimens were $\{1\,0\,0\}$ prisms ~ 4 mm long and ~ 2 mm × ~ 2 mm in cross-section. They were prepared by cleavage and coated with vacuum grease prior to testing. The grease served both to reduce the friction at the specimen/anvil interface and to protect the specimen against attack by atmospheric moisture.

Two variants of the experimental arrangement illustrated schematically in Fig. 1 were employed to measure the coefficient of friction. The first, installed in a glass environmental chamber, operated in nitrogen-rich air of controlled relative humidity at a pressure of ~ 10^5 Pa (1 atm); and the second operated at a pressure of 10^{-7} to 10^{-8} Pa in a bakeable stainless steel steel vacuum chamber. Even in the worst case of a sticking coefficient of one, when the entire flux incident upon a surface is adsorbed, the time to form a monolayer on a surface newly created in this latter environment is 1 to 10 h [27].

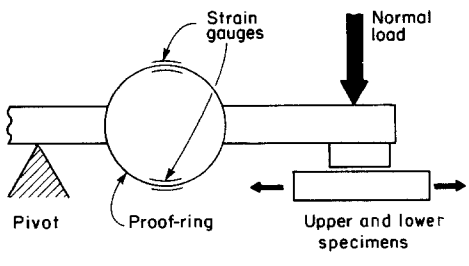

Figure 1 Schematic diagram of apparatus for measuring the coefficient of friction.

In both arrangements, the smaller (upper) specimen typically had a bottom face measuring ~ 3 mm $\times \sim 3$ mm and the larger (lower) specimen typically had a top face measuring 1 to 2 cm $\times \sim 5$ mm. Always both specimens (A and B) were oriented with a $\{1\,0\,0\}$ plane parallel to the (horizontal) contact interface and a $\langle 1\,0\,0\rangle$ axis parallel to the sliding direction, resulting in so-called $\{1\,0\,0\}_A\langle 0\,1\,0\rangle_A \parallel \{1\,0\,0\}_B\langle 0\,1\,0\rangle_B$ sliding. The smaller specimen was attached to the underside of one end of a freely pivoting horizontal balance arm which incorporated a proof-ring instrumented with four strain gauges in a full Wheatstone bridge arrangement; and the larger specimen was mounted on a motor-driven stage which automatically traversed it to and fro' parallel to the axis of the balance beam. Typically, the amplitude of this motion was a few millimetres and the sliding velocity was 0.2 to 0.6 mm sec^{-1}, giving a period ranging from a few seconds to more than 1 min.

An important prerequisite in such an experiment is that the surfaces of the two halves of the friction couple should (i) be aligned parallel to within an angle $\theta < \tan^{-1}(h/L)$, where h is the height of a typical asperity and L is the linear dimension of the nominal region of contact, and (ii) each be flat over its whole area to within a distance $< h$. Only when both these conditions are satisfied are the average number of asperity–asperity junctions per unit area and the average size of such a junction constant over the whole of the nominal area of contact.

In the present work, specimen alignment was provided by tilt and/or rotation adjustments built into the specimen carriages and the support for the pivot of the balance beam. The actual details differed between the two variants of the apparatus and are given elsewhere [28, 29]. Suffice it to note here that the alignment was carried out while monitoring the strain gauge indicator and observing the contact interface under strong back-lighting. Both the reading on the strain indicator and the amount of light transmitted through the gap between the specimens were least when the specimens were most nearly parallel. To obtain starting surfaces as flat as possible, the specimens were held tightly in a large, accurately machined, flat-ended holder made of hardened steel while they were polished to the requisite finish. This polishing operation was always carried out by hand, using as near-random a motion as possible in order to produce an isotropic surface topography. The resultant topography was studied by diamond stylus surface profilometry, optical microscopy and scanning electron microscopy, this last in the secondary electron mode of imaging. The same methods were also used to study the worn surfaces. In addition, transmission electron microscopy was used to study the wear debris produced. The profilometer stylus was a square pyramid with an angle of 90° between opposing face normals and tip radii of ~ 2.5 and ~ 7.5 μm parallel and perpendicular to its direction of travel.

Because friction arises from the making and breaking of discrete junctions between more-or-less mobile asperities, the force required to sustain sliding at a constant velocity must fluctuate with time. In the particular case of two parallel flat surfaces covered with micrometre-scale asperities which yield at a stress of (say) 3 MPa (see Section 3) to form junctions with an area of 1 μm^2, a simple calculation suggests that a load of 1 N and a sliding speed of (say) 0.3 mm sec^{-1} will lead to the formation of $\sim 3 \times 10^5$ junctions at any instant, each with a lifetime of ~ 3 msec. Neither of the present experimental arrangements had either the 1 part in 10^6 accuracy or the kiloHertz frequency response necessary to follow individual junction creation and annihilation under such conditions. Rather, when the output from the strain gauges was simply monitored with a chart recorder, the response was limited to an accuracy of ~ 1 part in 10^3 and a frequency of a few Hertz by the characteristics of that instrument; and, when the output was recorded and digitized under computer control, the response was more accurate but still limited to the natural frequency of the proof-ring under load. The two proof-rings involved had force constants of 8000 and 9000 N m^{-1}; and when a typical dead load of ~ 1 N was applied each had a mass of 150 to 200 g attached to it. Hence the natural frequency was 30 to 50 Hz in both cases. It therefore proved useful to incorporate into the computer-controlled data acquisition system a low-pass filter having a band width from 0 to 40 Hz of -3 dB. This had the effect of eliminating from the signal actually recorded all components having a frequency too high for them to have been generated by the strain gauges in response to events occurring at the contact interface.

Six series of friction measurements were carried out in all, with the first being designed to explore the effect on the coefficient of friction μ of (non-renewable) surface contaminants adsorbed during specimen preparation. In this first series, pairs of irradiated LiF crystals were successively polished on glass using slurries of 12 and 3 μm Al_2O_3 particles in water and on Buehler Texmet cloth (Buehler Ltd, Lake Bluff, Illinois) using 1 μm diamond paste in air of uncontrolled relative humidity. They were then tested in nitrogen-rich air at a relative humidity of $29 \pm 1\%$ both as-polished and following subsequent cleaning with hexane, toluene or paraffin oil. These solvents were chosen because the first leached the binder from the diamond paste, the second reacted with the paste to form a precipitate, and the third had no obvious effect on the paste. Each test was run for about 90 min, i.e. about 540 cycles of the sliding motion.

The second series of experiments was designed to look for any effect on μ of direct specimen exposure to water during preparation. In this case also, pairs of irradiated crystals were polished on glass with slurries of Al_2O_3; but now the smallest particles were 1 μm in size and the fluid was ethyl alcohol. Again, the testing was done in nitrogen-rich air at 30% relative humidity, but in this case the test time was increased to ~ 30 h (~ 1800 cycles).

The third series of experiments investigated the effects of initial surface roughness on friction. Measurements were made on pairs of irradiated LiF crystals which were polished on glass using one, two, three or all four of a series of aqueous slurries containing 25,

12, 3 or 1 μm particles of Al_2O_3. These tests were run for times ranging up to 40 h (~ 2400 cycles) in nitrogen-rich air at 30% relative humidity.

The influence of relative humidity on μ was the subject of the fourth series of experiments. Like pairs of irradiated LiF crystals were prepared as in the first series of experiments and then tested for ~ 90 min (~ 540 cycles) in nitrogen-rich air ranging in relative humidity from 10% to 100%. Note that, in contrast to the contaminants studied in the first series of experiments, the contaminant (water) adsorbed in this series is renewable and so capable in principle of affecting the frictional behaviour *ad infinitum*.

The influences of both environment and initial surface roughness on μ were studied in the fifth series of experiments. In this instance like pairs of irradiated LiF crystals were abraded on 600 grit (17 μm) SiC paper, rinsed in water, and cleaned ultrasonically in ethyl alcohol before being tested *in vacuo* for ~ 8 h (~ 500 cycles). The worn surfaces were then abraded manually *in vacuo*, using a steel file attached to a wobble-stick mounted on a bellows-type motion feed-through, before being tested for a further 8 h, reabraded, and so on.

The sixth and final series of experiments examined the effect on μ of varying yield strength at constant specimen composition. Like pairs of irradiated or annealed LiF crystals and unlike pairs consisting of one irradiated and one annealed LiF crystal were tested in nitrogen-rich air at 30% relative humidity for times up to 24 h (~ 1400 cycles). All of these samples were prepared in nitrogen-rich air of 23% relative humidity by polishing in turn on 600 grit (17 μm) SiC paper and with 12, 6, 3 and 1 μm diamond paste on Texmet cloth.

3. Results

Table I summarizes the results of the hardness and yield strength measurements. Note both the high ratio of Vickers hardness, H_v, to yield strength, σ_y, in compression and the much greater effect of irradiation on the latter as compared to the former.

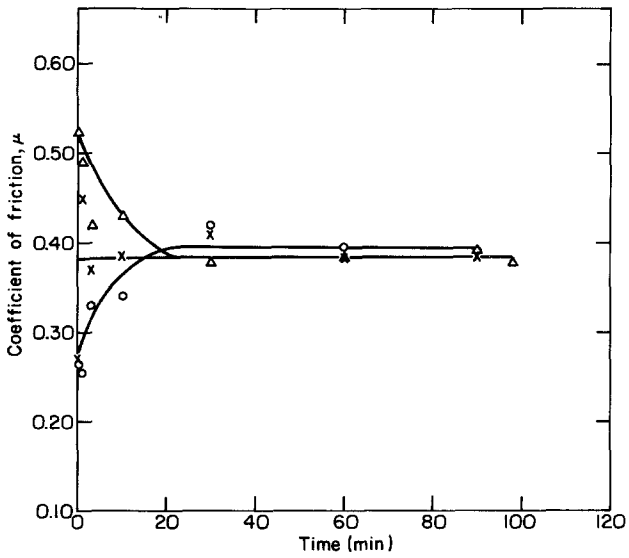

Figure 2 Influence of non-renewable surface contaminants on the coefficient of friction between two irradiated LiF crystals. (×) Hexane, (○) toluene, (△) paraffin oil.

Fig. 2 illustrates the effect on the frictional behaviour of like pairs of irradiated LiF crystals of different non-renewable surface contaminants adsorbed during specimen preparation. It is evident that the different reactions of hexane, toluene and paraffin oil with the binder in diamond paste lead to the formation of adsorbed layers with quite different tribological properties. It is also noteworthy that the effect of hexane, which dissolves the binder, is considerably shorter lived than the effects of toluene and paraffin oil, which do not. In all three cases, the coefficient of friction reaches a steady state value of 0.38 to 0.40 within ~ 20 min (~ 120 cycles). The same limiting value is also reached when the specimens are not exposed directly to water during surface preparation, Fig. 3.

TABLE I Vickers hardness and yield strength of LiF

	H_v (MPA)	σ_y (MPA)
Irradiated	1040	14.5
Annealed	918	4.2

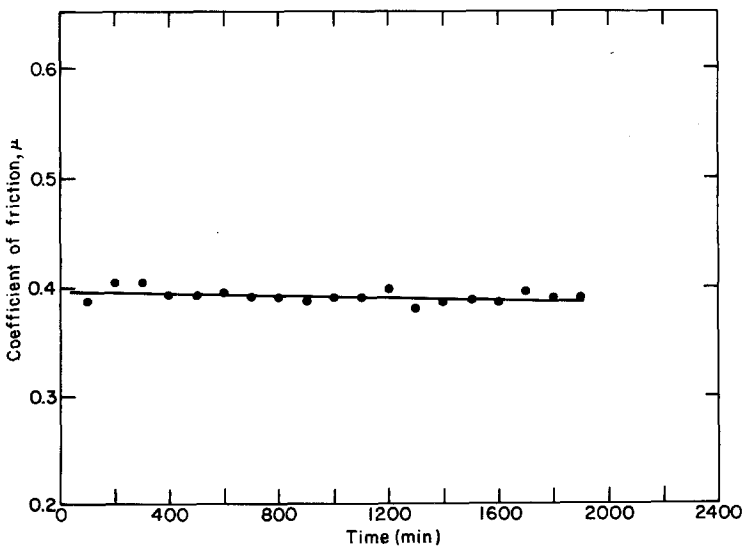

Figure 3 Variation of the coefficient of friction with time for a like pair of irradiated LiF crystals prepared without direct exposure to water.

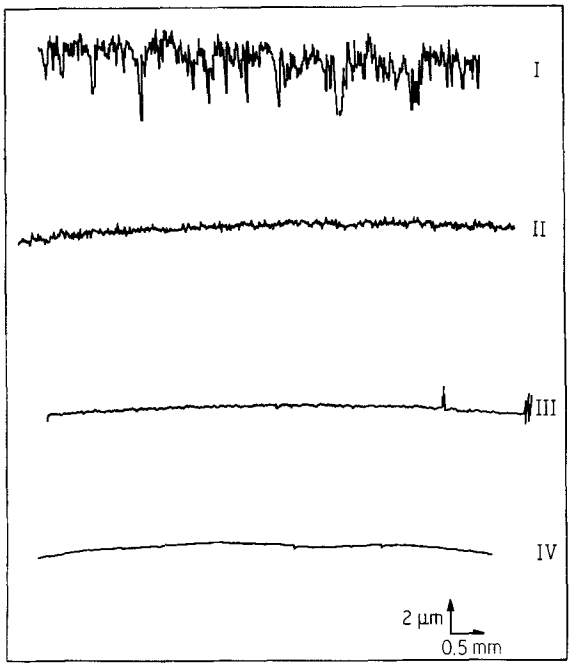

Figure 4 Surface profiles of as-prepared irradiated LiF crystals abraded with aqueous slurries containing 25, 12, 3 or 1 μm particles of Al_2O_3 (cases I to IV, respectively).

The irradiated LiF specimens used to study the effects of initial surface roughness on the coefficient of friction were abraded at their final stage of surface preparation with slurries containing 25, 12, 3 or 1 μm particles (cases I to IV, respectively). Profilometer traces of the resultant topographies are shown in Fig. 4, and Fig. 5 presents corresponding scanning electron micrographs. The traces reveal two things: first, that the average heights of the asperities generated in cases I to IV were ~ 1.3, ~ 0.5, ~ 0.15 and ~ 0.05 μm, respectively, i.e. ~ 0.05 times the size of the abrasive particles used to produce them; and second, that in cases II to IV, at least, the polished surfaces are not quite flat, but have a central dome ~ 1 μm in height. In addition, the scanning electron micrographs from cases I to III suggest that the asperities produced by the three coarsest abrasives have lateral dimensions comparable with the dimensions of the particles which produced them. Fig. 5 also suggests that cleavage played a more important role in asperity formation in case I than in case IV.

The frictional behaviour of like pairs of the surfaces illustrated in Fig. 5 decreased in consistency as their initial roughness increased. Nevertheless, when an

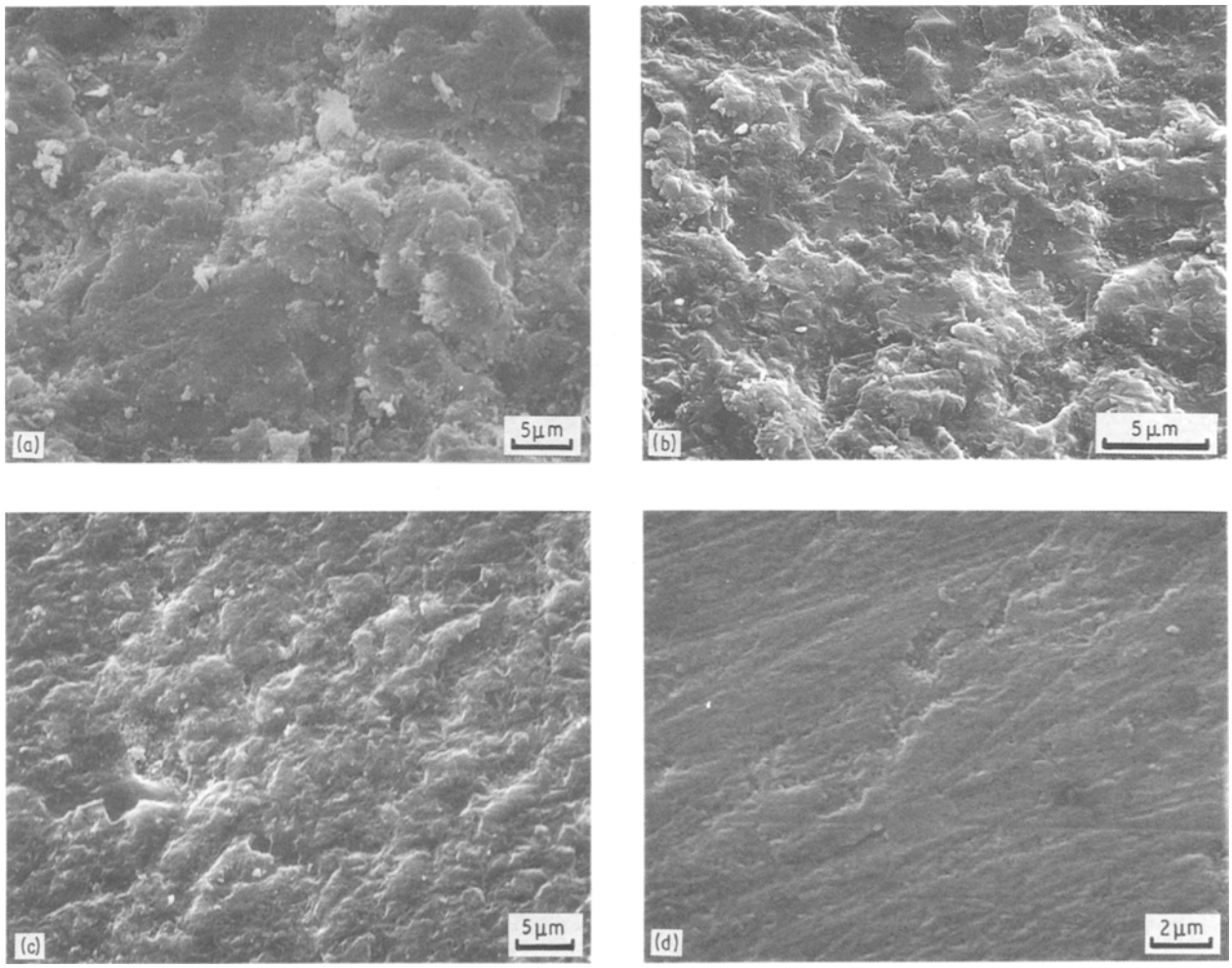

Figure 5 Scanning electron micrographs corresponding to the profiles shown in Fig. 4(a) to (d) illustrate cases I to IV, respectively.

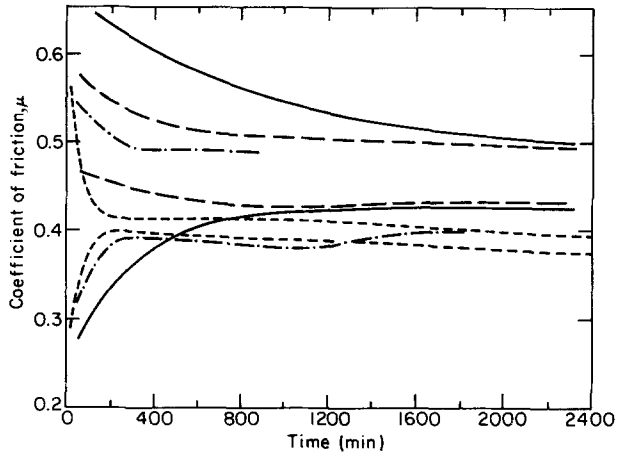

Figure 6 Variation of the coefficient of friction during running-in for several like pairs of irradiated LiF crystals. Cases (—) I, (– – –) II, (—·—) III, (– – –) IV.

experiment ran long enough, the coefficient of friction always tended asymptotically to ~ 0.4. Fig. 6 shows the upper and lower limits to the full range of values of μ observed in many different tests for each of cases I to IV. It is evident that the process of "running in" takes longer for surfaces which are initially rougher, and that for such surfaces the coefficient of friction generally varies more widely during this process. It is also evident that the initial value of the coefficient of friction may be either higher or lower than the asymptotic value.

No correlation could be discerned between the value of the coefficient of friction at any instant and the concurrent size or shape of the apparent area of contact as indicated by the wear scar on either specimen, even though the geometry of both scars varied widely in the early stages of sliding due to the slightly domed shapes of the starting surfaces. After sliding for very long times, however, the wear scar on the smaller (upper) specimen frequently did grow to cover the entire lower surface of that specimen. Concomitantly, the wear scar on the upper surface of the larger (lower) specimen usually grew to the size and shape expected from the dimensions of the upper specimen and the amplitude of the sliding motion. Figs 7a and b show portions of such a well-developed scar on a larger (lower) specimen at two different magnifications. Typically, the coefficient of friction reached its asymptotic value before the wear process developed thus far.

Other highly variable features of wear scar morphology were the amount of wear debris adhering to the grooves formed parallel to the sliding direction, the amount of debris ejected from the contact interface on to the undamaged regions surrounding the wear scar on the lower specimen, and the degree of consolidation of the debris in both regions. Some indication of this variability is apparent in Fig. 8, which shows a wear scar produced on a case II starting surface after 12 h sliding. Note the large, partly detached, plate-shaped mass of wear debris at top right, the "clean" grooves to its left, the smaller plate-like masses of debris at top left, and the less heavily worn area at lower right. Examination of the large mass at higher magnifications, Fig. 9, shows that it consists of densely packed debris particles, most of which appear to be in the 100 nm size range, Fig. 9d. This mass also is grooved in some places, Fig. 9b, and fractured in others, Fig. 9c. Fig. 10a is another high magnification micrograph showing the well-defined grooves immediately to the left of the same mass, Fig. 8. Only a few 100 nm scale particles, and even fewer aggregates of such particles, remain attached to the worn surface in this region. In the top left-hand corner of the scar, Fig. 8, numerous smaller plate-like masses of debris apparently adhere strongly. These are shown at high magnification in Fig. 10b. Portions of the starting surface are visible between these masses, albeit they are partly obscured by loose debris particles which have not yet been packed together. The less heavily worn area in the lower right-hand corner of the scar seen in Fig. 8 is shown at higher magnification in Fig. 10c. This last figure reveals that the wear particles formed early in the wear process range downwards in size from ~ 1 μm. Correspondingly, the absence of particles as large as 1 μm from Figs 9b, c, and d suggests that extensive particle comminution occurs as the particles are compacted into plate-like masses.

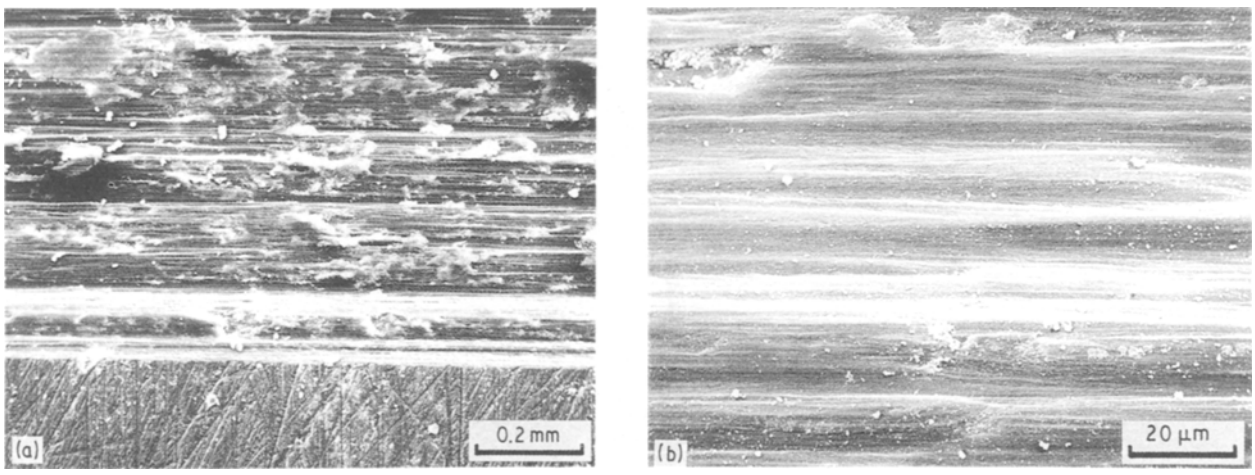

Figure 7 Well-developed wear scar on the lower member of a friction couple consisting of two irradiated LiF crystals, as seen at two different magnifications.

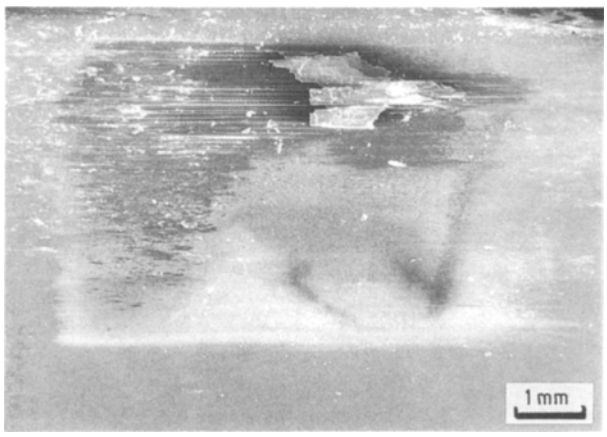

Figure 8 Wear scar produced on the lower member of a friction couple consisting of two irradiated LiF crystals by sliding for 12 h. Case II.

Studies of the wear scars created on cases I, III and IV starting surfaces reveal the same features – grooved areas more-or-less free of debris particles, areas covered by more-or-less well-attached plate-like masses of densely packed 100 nm scale debris particles, and areas partially obscured by more-or-less densely packed such particles. Figs 11a and b are bright-field transmission electron microscope images of debris particles generated from cases I and IV starting surfaces, respectively. They confirm that the individual particles are remarkably consistent in size, with an average dimension of 100 nm or less. Some of those formed from the case IV starting surface have a cuboid habit, suggesting that they were formed by cleavage and/or extensive shear on {1 0 0}, while others are more rounded or irregular in shape; but all are equiaxed. More of those formed from the case I starting surface are irregular in shape, but again they are all equiaxed. None of the particles exhibits any contrast indicating the presence of a dislocation.

Such fine particles have a large surface-to-volume ratio and thus may be expected to react quickly with their environment. This raises the question of whether particles produced under conditions of controlled relative humidity might undergo a solution–reprecipitation reaction as a result of being exposed first to more humid air during transfer to the scanning or transmission electron microscope and then to a hard vacuum prior to being imaged. In the case of LiF, however, its solubility in water at room temperature is low enough ($\sim 5 \times 10^{-4}$ mole l^{-1} [30]) that the water should obey Raoult's Law. Hence, the vapour pressure of water over even a saturated aqueous solution of LiF should be $> 99.9\%$ of that of pure water, and there should be no tendency for water in the

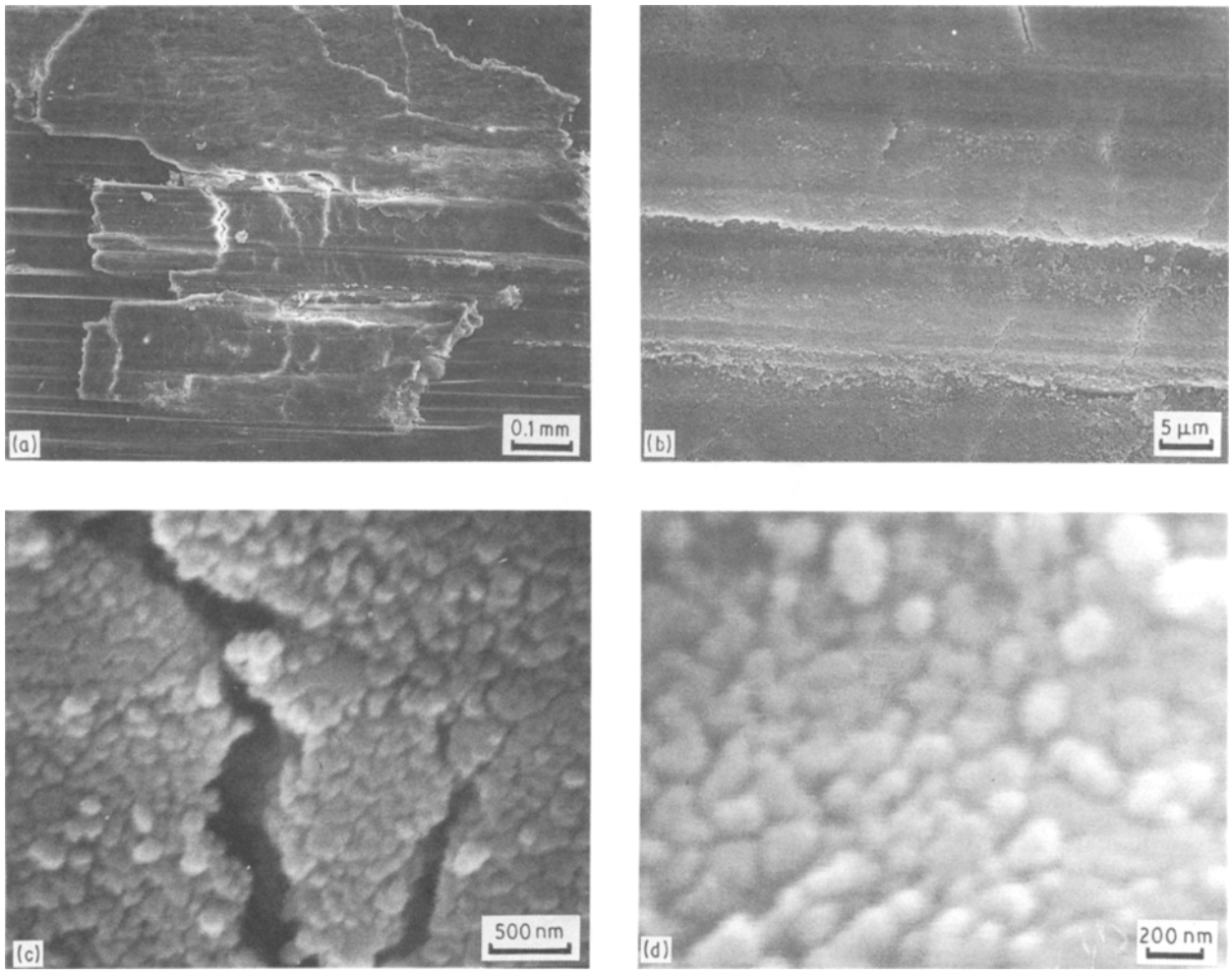

Figure 9 The large plate-like mass of well-consolidated debris particles shown in Fig. 8. (a) Overview, (b) longitudinal grooves, (c) internal fractures, and (d) constituent debris particles at high magnification.

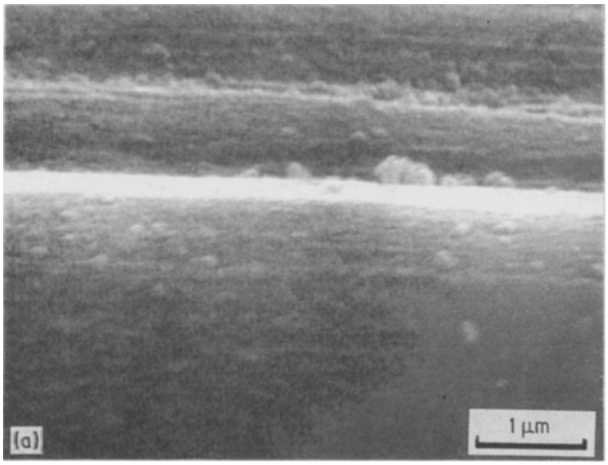

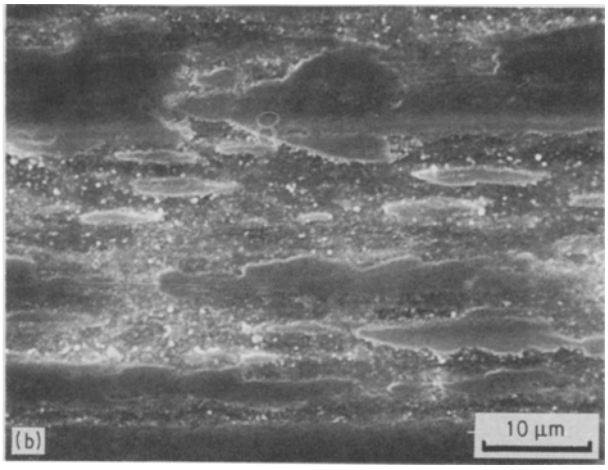

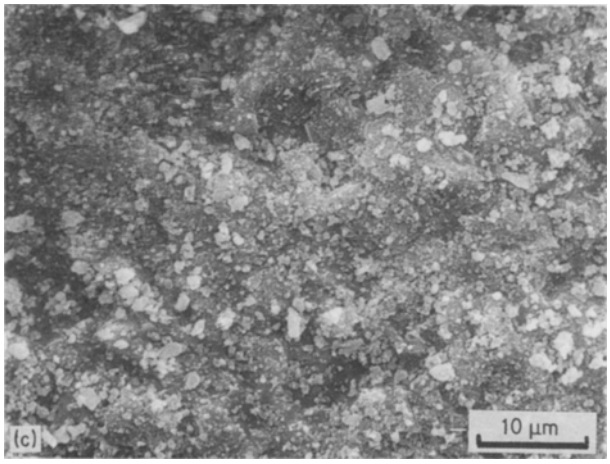

Figure 10 Regions of the wear scar shown in Fig. 8. (a) Immediately to the left of the feature shown in Fig. 9, (b) far to the left of this feature, and (c) in the lower right-hand corner. At (a) little debris adheres to the wear grooves; at (b) numerous small plate-like masses of debris particles apparently adhere strongly; and at (c) the debris is larger and more loosely consolidated.

atmosphere to react with the debris particles unless the relative humidity were to exceed 99.9%. Except when measuring the coefficient of friction in saturated nitrogen-rich air (see below and in Figs 13 and 14), this did not happen in the present work.

Fig. 12 shows profilometer traces recorded perpendicular to the wear grooves formed on cases I to IV starting surfaces after ~ 12 h sliding. All four surfaces have undergone appreciable amounts of wear, in the course of which the roughest starting surface (case I) appears to have become smoother and the three smoother surfaces (cases II to IV) to have become rougher. Note also that the depths of the grooves appear to be greater on the latter three surfaces than on the former. Perhaps the most telling observation in Fig. 12, however, is that the ridges between some of the grooves rise above the original surface. When considered together with the evidence of extensive comminution of debris presented in Figs 9 to 11, this observation suggests that such ridges are formed from debris particles so firmly compacted together that the stylus of the profilometer could not penetrate through to the intact material beneath. It follows that all of the deductions drawn above from Fig. 12 must be regarded as tentative.

The fourth series of experiments, which investigated the effect of relative humidity on the frictional behaviour of like pairs of irradiated LiF crystals, showed that the coefficient of friction approached an asymptotic value dependent on the relative humidity after 20 to 40 min (20 to 40 cycles). Hence, it was possible to construct the time-independent plot shown in Fig. 13, which illustrates that the frictional behaviour of such a couple does not depend markedly on relative humidity. The coefficient of friction was ~ 0.40 at saturation, fell slowly to a shallow minimum of ~ 0.38 at ~ 50%

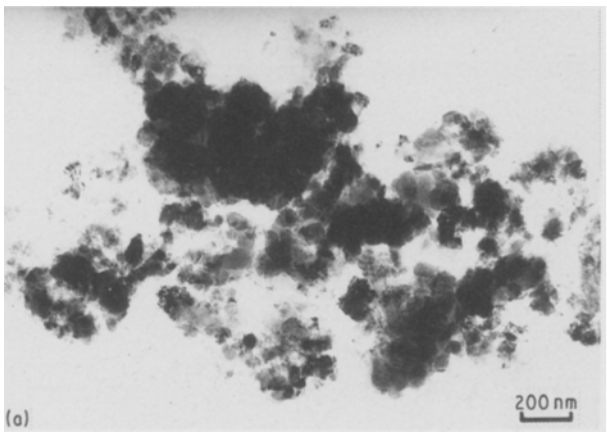

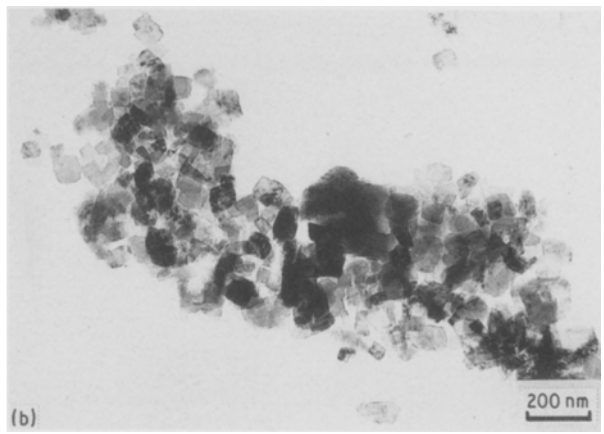

Figure 11 Bright-field transmission electron microscope images of debris particles. (a) Case I, and (b) case IV.

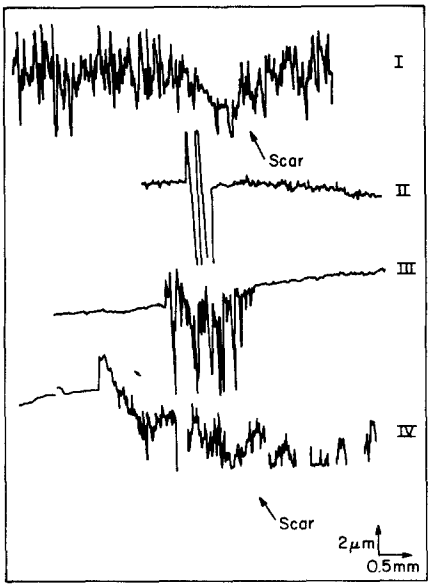

Figure 12 Profiles of wear grooves formed by one irradiated LiF crystal sliding to and fro' on another for ~ 12 h. Cases I to IV.

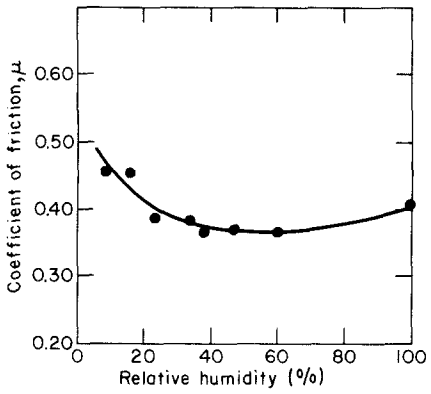

Figure 13 Variation of the limiting value of the coefficient of friction with relative humidity for a like pair of irradiated LiF crystals.

relative humidity, and then rose a little more steeply at relative humidities $\lesssim 20\%$. Note that at a relative humidity of 30% the coefficient of friction was again ~ 0.40. Only very close to saturation did relative humidity affect the morphology of the wear scar. Fig. 14 suggests that under such conditions the debris particles were larger (a few hundred rather than 100 nm), less closely packed together, and more uniformly distributed over the scar. This change in morphology is thought to be the result of dissolution of fine debris particles during sliding followed by re-precipitation during evacuation of the microscope prior to switching on the electron beam.

The results of the fifth series of experiments are important for two reasons. First, they show that the coefficient of friction for one irradiated LiF crystal sliding on another has the same value (0.42 to 0.45) in ultra-high vacuum as in fairly dry nitrogen-rich air (relative humidity $\lesssim 15\%$, Fig. 12) at a pressure twelve orders of magnitude higher. Fig. 15 presents data obtained at a pressure of 7.5×10^{-8} Pa from specimens prepared either by filing in air prior to pump-down or by filing *in vacuo*. (The lack of evidence in this figure of running-in is thought to be fortuitous.)

The second important result of these experiments is illustrated in Fig. 16, which shows data obtained from a pair of irradiated LiF crystals sliding in air of 50% relative humidity. The starting surfaces were in this case prepared by abrading on 600 grit (17 μm) SiC paper as described in Section 2.2. The data in Fig. 16 were collected and analysed under computer control, a process at once less subjective and less restricted in both accuracy and frequency response (see Section 2.2) than averaging the output from a chart recorder by hand. Each datum point is the average of 8000 values of the coefficient of friction collected at a rate of 800 points per cycle of sliding over the first 10 consecutive cycles of every 50. The error bars, which indicate ± 1 S.D., vary systematically in extent because the low-pass filter was alternatively switched on and off during successive (10 cycle) periods of data collection until 400 cycles of sliding had accumulated (in ~ 400 min). Thereafter, the data were filtered at amplifications ranging from ~ × 200 to ~ × 4 for the remainder of the test. The results show a typical initial transient, this time ~ 100 cycles in length, during which the coefficient of friction rises to a steady value of 0.40. They also show that the friction measuring system did pick up extraneous noise, that

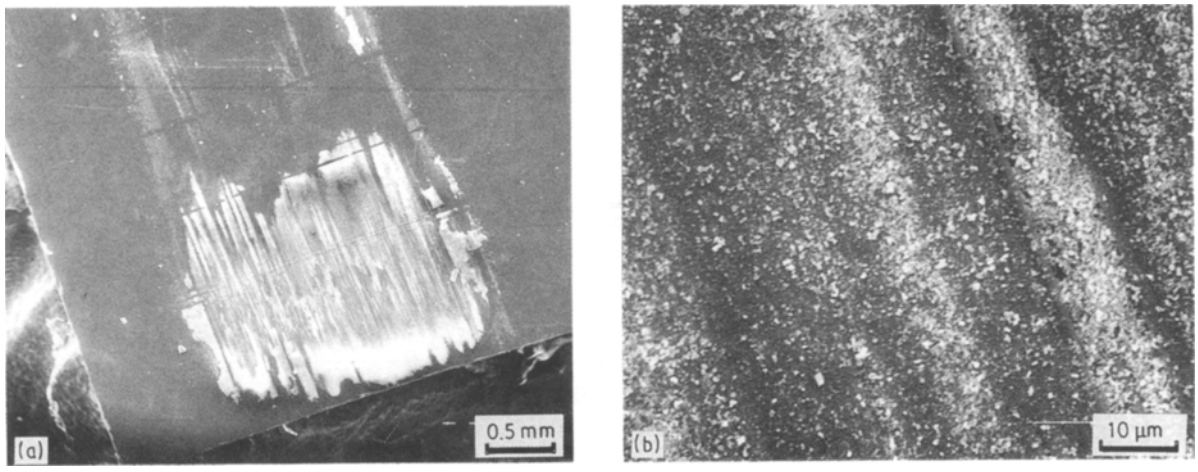

Figure 14 Wear scar formed on one irradiated LiF crystal by sliding against another in nitrogen-rich air saturated with water vapour.

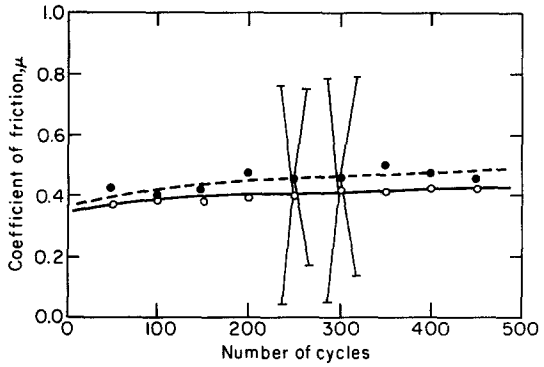

Figure 15 Variation of the coefficient of friction with time for differently prepared like pairs of irradiated LiF crystals sliding in ultra-high vacuum (a pressure of $\sim 7.5 \times 10^{-8}$ Pa). Filed in (○) air, (●) *in vacuo*.

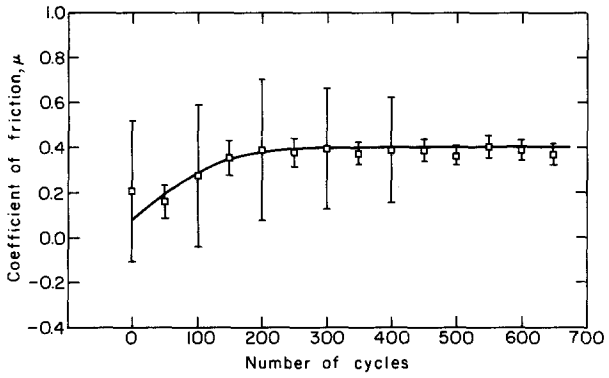

Figure 16 Effect of low-pass filtering and amplification on the measurement of the coefficient of friction under computer control.

this noise was random and could be eliminated without affecting the mean value of the coefficient of friction, and that the different accuracies and frequency responses of the two data collection systems involved in this work did not lead to inconsistent results.

The results of the sixth and final series of experiments are presented in Fig. 17. These show that, when one LiF crystal is slid over another in nitrogen-rich air at a relative humidity of 30%, the coefficient of friction is always in the range 0.38 to 0.40, regardless of whether both crystals are annealed, one is annealed and the other irradiated, or both are irradiated. To demonstrate the consistency of the last part of this result, the line presented in Fig. 17 for irradiated pairs of crystals was obtained by averaging together all the data obtained from such pairs at this relative humidity throughout the study, regardless of initial surface roughness and contamination. The error bars again represent $\pm$ 1 S.D., and their rapid diminution with time is graphic evidence of the development of a wear surface topography characteristic of the test protocol and independent of the method of specimen preparation. In all three cases both the worn surfaces and the debris particles adhering to them exhibited the same features as those shown in Figs 8 to 11.

4. Discussion

The striking result of this work is that, regardless of relative humidity, initial surface roughness and con-

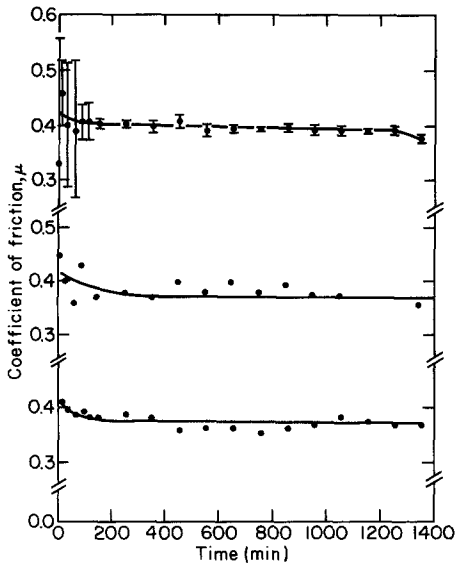

Figure 17 Variation of the coefficient of friction with time for three different pairs of LiF crystals in nitrogen-rich air at a relative humidity of 30%. Upper curve, both crystals irradiated; middle curve, one crystal irradiated and the other annealed; lower curve, both crystals annealed.

tamination, and of whether either or both of the crystals be annealed or irradiated, the steady-state coefficient of friction for two LiF single crystals A and B sliding in $\{1\,0\,0\}_A \langle 0\,1\,0\rangle_A \| \{1\,0\,0\}_B \langle 0\,1\,0\rangle_B$ orientation is always in the range 0.42 ± 0.04.

The effects of non-renewable contaminants on the coefficient of friction do not persist beyond about 100 cycles of the sliding motion, i.e. a cumulative relative displacement $\lesssim 0.1$ m, and the effects of even micrometre-scale initial surface roughness disappear by the time this displacement rises to a few metres.

The coefficient of friction also varied but little in the presence of different renewable concentrations of water vapour, rising from a minimum of ~ 0.38 at a relative humidity of 50% to ~ 0.45 at relative humidities less than $\lesssim 15\%$ and in ultra-high vacuum. Such variation is smaller than the reported effects of water on the indentation hardness of LiF [13, 14, 18] and on the mobilities of individual primary ($\{1\,1\,0\}\ \langle 1\,\bar{1}\,0\rangle$) edge and screw glide dislocations about hardness impressions in this material [19, 20]; but it is difficult to compare quantitatively with the reported effects of water on the glide and multiplication of the same dislocations during a single passage of a lightly loaded sapphire slider over the surface of such a crystal [15–17, 21].

The present work further shows that irradiation hardening a single crystal of LiF, which increased its yield strength in $\langle 1\,0\,0\rangle$ compression by a factor $\times$ 3.5 but its Vickers hardness only by a factor $\times$ 1.1, had no effect on its frictional behaviour.

Both the very different effects of irradiation on yield strength and hardness and the very high ratio of hardness to yield strength are usually explained in terms of plastic anisotropy. In $\langle 1\,0\,0\rangle$ compression the yield strength is simply twice the critical resolved shear stress $\tau_y\{1\,1\,0\}$ for primary glide. Such glide is easy in an annealed crystal of high purity because the

Peierls–Nabarro stress opposing dislocation motion on $\{1\,1\,0\}$ is low; but it is made difficult in an irradiated crystal by interaction of the dislocations with the colour centres created by the radiation. Hence, the yield stress is sensitive to irradiation. In contrast, it is argued, formation of a hardness impression requires both primary and secondary ($\{1\,0\,0\}\langle 1\,\bar{1}\,0\rangle$) glide to accommodate the more complex shape change involved, and hence hardness should be controlled by the much higher critical resolved shear stress $\tau_y\{1\,0\,0\}$ for secondary glide [31, 32]. This latter is always determined by the Peierls–Nabarro resistance to dislocation motion on $\{1\,0\,0\}$ ([6] p. 21, [33]), which at ambient temperatures far exceeds the strength of any dislocation–point defect interaction. It then follows that hardness should be but little affected by irradiation, in accord with experiment.

Attractive though this argument is, it is not yet supported by direct evidence of the occurrence of secondary glide during indentation of LiF. It is also difficult to reconcile with several other observations. One is that the Vickers hardnesses of the $\{1\,0\,0\}$, $\{1\,1\,0\}$ and $\{1\,1\,1\}$ surfaces of LiF are the same, to within experimental error [34], even though uniaxial compression along $\langle 1\,0\,0\rangle$ stresses only (some) primary glide systems and similar compression along $\langle 1\,1\,1\rangle$ stresses only (some) secondary glide systems. A second is that the variation of Knoop hardness on $\{1\,0\,0\}$ with change of indentor orientation can be explained qualitatively (though not quantitatively) in terms of primary glide alone [35–38]. Finally, the value (~ 95 MPa) of $\tau_y\{1\,0\,0\}$ measured by Liu and Skrotzki [39] in $\langle 1\,1\,1\rangle$ compression at a strain rate of $10^{-4}\,\mathrm{sec}^{-1}$ and a temperature of 295 K seems too low for this stress to be the sole determinant of the hardness [31, 40, 41]. Nor does it seem plausible that either the comparatively high rate of strain ($\sim 10^{-2}\,\mathrm{sec}^{-1}$) or the large hydrostatic compression occurring beneath an indentor during an indentation test could raise $\tau_y\{10\}$ sufficiently to eliminate the discrepancy [39, 42, 43]. To generate stresses of the magnitude (300 to 500 MPa, or about one-tenth of the theoretical shear strength ([7] p. 32)) necessary to account for the observed hardness of LiF by the action of dislocations requires that adjacent (like) dislocations be forced to close to within 3 to 5 nm, or about the probable width of their cores [44–46]. This suggests that the ultimate determinant of the hardness of LiF is not the lattice resistance to glide on $\{1\,0\,0\}$, but rather the stress necessary to force intersecting primary slip bands to interpenetrate instead of initiating fracture (as is normal in the absence of sufficient hydrostatic pressure). This stress should likewise be insensitive to irradiation.

Plastic anisotropy also seems an unlikely explanation for the observed insensitivity of the coefficient of friction to irradiation. In this connection, it is significant that both the debris particles produced from annealed crystals of particular initial surface roughness in a particular environment and those produced from irradiated crystals of varying initial surface roughness in different environments are devoid of all dislocations, primary or secondary.

A free surface exerts an attractive image stress

$$\sigma_i \sim Gb/4\pi x \qquad (1)$$

on a dislocation with a Burgers vector of magnitude b situated a distance x below it in a solid of shear modulus G [47]; and hence any particle of linear dimension

$$d_{\min} \lesssim Gb/2\pi\tau_y\{h\,k\,l\} \qquad (2)$$

is unlikely to retain any dislocation which glides at a critical resolved shear stress $\tau_y\{h\,k\,l\}$. Now, for LiF the lattice parameter $a_0\langle 1\,0\,0\rangle = 0.401$ nm [48], so that $b = 0.284$ nm, $G\{1\,1\,0\}\langle 1\,\bar{1}\,0\rangle$ and $G\{1\,0\,0\}\langle 1\,\bar{1}\,0\rangle$ are 33 and 58 GPa, respectively ([6] p. 20, [7] p. 389, [49]), $\tau_y\{1\,1\,0\} = \sigma_y/2$ is 7.3 MPa for an irradiated crystal and 2.1 MPa for an annealed one, Table I, and $\tau_y\{1\,0\,0\} = 95$ MPa [39]. Substitution of these values into Inequality 2 predicts that debris particles formed from annealed and irradiated crystals will cease to retain primary dislocations once $d_{\min}$ falls below ~ 710 and ~ 205 nm, respectively, but will not lose secondary dislocations until $d_{\min}$ falls to less than ~ 28 nm.

The action of image forces thus provides a convincing explanation for the absence of primary dislocations from the ~ 100 nm particles shown in Figs 11a and b, but the same action cannot be held responsible for the absence of secondary dislocations. Rather, it has to be concluded that these latter dislocations were never formed in appreciable numbers. This last conclusion is at first sight surprising, given that the overall deformation imposed on the immobile asperities at the contact interface, i.e. shear on $\{1\,0\,0\}$, cannot be produced by primary glide alone. It can, however, be rationalized by arguing that the local deformation resulting from contacts between asperities, whether mobile or immobile, occurs via some other mode which is compatible with primary glide, i.e. the flow at the contact interface is turbulent rather than laminar.

Implicit in this discussion is the assumption that primary glide is as essential a precursor to the formation of wear debris as it is to any other fracture process in LiF. When this material is deformed plastically at room temperature, dislocation glide occurs mostly on $\{1\,1\,0\}$, but dislocation multiplication occurs by line segments of screw orientation cross-gliding first on to $\{1\,0\,0\}$ and then back on to $\{1\,1\,0\}$ parallel to their original glide planes [50]. Because the edge segments left on $\{1\,0\,0\}$ are highly immobile, the net result is the creation of many Frank–Read sources on parallel $\{1\,1\,0\}$ planes. This leads to the formation of slip bands which widen as they grow. Typically, a few such bands originate at surface steps and then develop until they penetrate the bulk of the crystal. Within a growing band the dislocation density remains constant at a saturation value which ranges from $\sim 1 \times 10^{11}\,\mathrm{m}^{-2}$ for a soft crystal of high purity deformed at room temperature to $\sim 3 \times 10^{11}\,\mathrm{m}^{-2}$ for a crystal hardened by irradiation, by cooling to cryogenic temperatures, or by doping with aliovalent impurities [50]. Note in passing that, if dislocation density tends to the same limits in the present experiments, only one in three of the "original" micrometre-size debris particles produced from irradiated crystals and one in ten of those produced from annealed crystals would contain any

dislocation for the image forces to remove. These numbers seem unreasonably low if debris particle formation is indeed the result of primary glide-induced fracture. The implication is that the greater hydrostatic constraint in sliding contact as compared to uniaxial compression leads to the attainment of higher dislocation densities prior to the nucleation of cracks.

As the growing bands begin to impinge on one another, dislocations pile up on intersecting slip planes, generating large local tensile stresses and initiating fracture. Further cracking then ensues with increase in strain, and eventually these cracks link up to cause fracture. Because crack nucleation is a statistical process, governed both by the number of sources available to form glide bands [51] and by the way in which the development of these bands is constrained by specimen geometry [52], the strain to failure is widely variable [53, 54].

Both the rate of work-hardening (in particular the extent of easy glide) and the fracture stress are subject to corresponding statistical variation. Typically, however, the yield stress of an annealed crystal of high purity deformed in $\langle 1\,0\,0\rangle$ compression rises by 1 to 2 MPa for each 1% increment of strain until fracture occurs at a stress of 30 to 40 MPa [53, 54]. Irradiation raises the yield stress and decreases the strain to fracture, but it has less effect on the work-hardening [54].

It thus seems plausible that wear debris formation in LiF should begin via some sort of (primary) glide-induced fracture process, with cracks forming at the contact interface and intersecting to detach particles which immediately lose the near-surface part of their dislocation content to the action of image forces. Subsequent breakage of these particles into smaller fragments results in further loss of dislocations, and the evidence in Figs 11a and b is that this process proceeded to its logical conclusion in the present experiments.

As long as a debris particle contains dislocations which can glide on intersecting glide planes, it can, in principle at least, continue to break by propagation of a crack nucleated by blockage of glide; and, if it contains even a single source of glissile dislocations, it can in principle separate into two parts by shear. Alternatively it can fail by (brittle) propagation of either a pre-existing crack or a crack introduced as contact damage. Once it is free of cracks and dislocations, however, further fragmentation requires the nucleation of fresh dislocations at the theoretical shear strength. (Because debris particles experience dominantly compressive loading, the nucleation of new cracks at the theoretical tensile strength is deemed unlikely). The most plausible location for such dislocation nucleation is within the region of concentrated stress associated with surface steps [55, 56]. In the absence of any mechanism for stress concentration, the applied stress must itself reach the theoretical shear strength throughout the entire volume of the debris particle. A further important consideration is that, when further comminution of the particles becomes too difficult, sliding can occur by their riding over or past one another as near-rigid bodies, i.e. with their deformation remaining purely elastic. Where the problem is treatable, it is instructive to analyse the mechanics of these various processes, bearing in mind that those which operate only at stresses much greater than that necessary to drive dislocations past F centres ($\sim$ 7 MPa in the present work, Table I) are unlikely to exhibit much sensitivity to irradiation.

Stroh [57] estimated the resolved shear stress, τ, necessary to nucleate a crack at the head of a pile-up of dislocations of length, L, as

$$\tau = [3\pi\gamma G/8(1-\nu)L]^{1/2} \quad (3)$$

where γ is the energy of the new surface produced and ν is Poisson's ratio. Setting $\gamma = \gamma\{1\,0\,0\} = 0.42\ \mathrm{J\,m^{-2}}$ [58–60], $\nu = 0.30$ ([6] p. 20, [7] p. 39, [49] $G = G\{1\,1\,0\}\langle 1\,\bar{1}\,0\rangle = 33$ GPa, and $L = d_{\min}/2$ yields $d_{\min} = 150$ μm for an annealed crystal work-hardened to the point of fracture ($\tau = \tau_y = 17.5$ MPa, say). This is two orders of magnitude larger than the linear dimension ($\sim$ 1 μm) of the largest debris particle seen in the present work. To produce micrometre-scale particles via this mechanism requires that τ_y reach $\sim$ 200 MPa, and to produce an 100 nm particle requires $\tau_y \gtrsim$ 600 MPa. The former is about half the level of stress thought to be reached beneath a Vickers diamond pyramid indentor, and the latter exceeds this level. The ultimate determinant of the onset of debris particle formation may therefore be the same as the ultimate determinant of hardness, namely the stress necessary to force intersecting slip bands to interpenetrate under hydrostatic constraint. In sliding contact, however, the hydrostatic constraint presumably is lower than during a hardness test because an asperity composed of LiF is softer and more compliant than an indentor made of diamond; and so fracture occurs at a lower level of shear stress.

To shear a particle into two parts by repeated operation of a single Frank–Read source, or by the related process of multiple cross-glide, requires that the ends of each (unstably) expanding loop meet and annihilate (and thereby regenerate the source) before the rest of the loop is lost to the action of image forces. This suggests that the length of the source could not be greater than $\sim d_{\min}/3$; and hence the stress τ_d required to operate it is

$$\tau_d \sim 3Gb/d_{\min} \quad (4)$$

where G is the appropriate shear modulus and b of the Burgers vector [47, 61]. Taking $d_{\min} = 1$ μm, $b = 0.284$ nm, and $G = G\{1\,1\,0\}\langle 1\,\bar{1}\,0\rangle = 33$ GPa yields $\tau_d = 28$ MPa; and for 710 nm and 205 nm particles the same equation predicts $\tau_d = 40$ MPa and $\tau_d = 135$ MPa, respectively. Like the stresses obtained from Equation 3, these stresses are all significantly greater than those generated either by lattice resistance to primary glide or by interaction of primary dislocations with irradiation-induced point defects.

The alternative to shearing a particle apart is to fracture it. For this to happen in compression by propagation of a pre-existing flaw prior to general yielding requires [62–64]

$$d_{\min} \geq 11E\gamma/\sigma_y^2 \quad (5)$$

Substituting $E\langle 1\,0\,0\rangle = 84$ GPa ([6] p. 20, [49]), $\gamma\{1\,0\,0\} = 0.42\,\mathrm{J\,m^{-2}}$ [58, 80], and $\sigma_y = 2\tau_d = 80$ and 270 MPa for annealed and irradiated material, respectively, yields $d_{min} = 60$ and 5 μm. Both values are significantly greater than the linear dimension of the smallest particle likely to retain a primary dislocation capable of acting as a Frank–Read source. If the particle is dislocation-free, it will yield when $\tau_y = 2\tau_{th}$, where τ_{th} is the theoretical (shear) strength for shear on the primary glide plane parallel to the primary glide direction. This strength should not be affected by irradiation as long as the dose remains low enough that the average particle contains only individual F centres rather than aggregates of (say) $> 10^2$ to 10^3 such centres. This is believed to be the situation in the present experiments. As a first approximation, therefore, τ_{th} is taken as $G\{1\,0\,0\}\langle 1\,\bar{1}\,0\rangle/2\pi$ for both annealed and irradiated material ([7] p. 27), leading to $d_{min} = 14$ nm for each. These results suggest that debris particles derived from annealed or irradiated material and containing a pre-existing flaw will exhibit ductile-to-brittle transitions as their linear dimensions diminish below ~ 710 and ~ 205 nm, respectively, and they cease to retain primary dislocations. They also suggest that both kinds of particle will revert to ductile behaviour if they are reduced in size to $\lesssim 14$ nm.

Hagan [65] has considered the related question of the smallest particle which can sustain nucleation of a crack by elastically constrained plastic deformation during point-contact loading. He predicts

$$d_{min} \simeq 60\,E\gamma/H_v^2 \qquad (6)$$

leading to $d_{min} = 2.5$ μm for annealed LiF and $d_{min} = 2.0$ μm for irradiated LiF. This suggests that fresh cracks are unlikely to be introduced into the present debris particles as they undergo comminution at the sliding interface, regardless of whether they originate from annealed or irradiated material.

As has been pointed out by Rigney *et al.* [66], there also is a lower limit to the size of crack- and dislocation-free particle which can be made to fracture. This is set by the requirement that the stored elastic strain energy, which depends on d_{min}^3, exceed the energy of the new surface formed, which depends on d_{min}^2. Rigney *et al.* consider only tensile failure, but a more realistic prediction results if it is assumed that the particle shears off (homogeneously) on $\{1\,1\,0\}$ parallel to $\langle 1\,\bar{1}\,0\rangle$ in response to an uniform compressive stress $\sigma_c = 2\tau_{th} = G\{1\,1\,0\}\langle 1\,\bar{1}\,0\rangle/\pi$. For the near-cubical particles shown in Figs 11a and b, this argument leads to

$$\frac{\sigma_c^2\, d_{min}^3}{2\,E\langle 1\,0\,0\rangle} > 2\sqrt{2}\, d_{min}^2\, \gamma\{1\,1\,0\} \qquad (7)$$

or

$$d_{min} > 4\sqrt{2\pi^2\, E\langle 1\,0\,0\rangle\, \gamma\{1\,1\,0\}/G\{1\,1\,0\}\langle 1\,\bar{1}\,0\rangle^2} \qquad (8)$$

Substituting $E\langle 1\,0\,0\rangle = 84$ GPa, $G\{1\,1\,0\}\langle 1\,\bar{1}\,0\rangle = 33$ GPa and $\gamma\{1\,1\,0\} = 1\,\mathrm{J\,m^{-2}}$ [58] yields $d_{min} = 4.3$ nm. Thus, comminution of the present debris particles stopped well short of its theoretical limit in the present work. It is worth noting in passing, however, that debris particles as small as ~ 5 nm have been produced from both metallic [66] and ceramic materials [67].

In the case of a less regularly shaped crack- and dislocation-free particle, within which stress is distributed inhomogeneously and dislocation nucleation occurs wherever $\tau\{1\,1\,0\}\langle 1\,\bar{1}\,0\rangle$ first reaches $G\{1\,1\,0\}\langle 1\,\bar{1}\,0\rangle/2\pi$, the corresponding value of d_{min} will necessarily be greater than 4.3 nm; but it is very difficult to obtain a numerical estimate for particles of anything but the very simplest of shapes.

Even more difficult to estimate is when sliding will cease to occur by the debris particles fracturing or deforming via dislocation glide and multiplication and start to occur by these particles riding over or past one another as near-rigid (elastic) bodies. Nor is it easy to estimate what the coefficient of friction would then be, though it would not be expected to be sensitive to irradiation.

5. Conclusions

While care needs to be taken not to attach too much significance to the preceding calculations, their results do throw some light on the probable mechanism of formation of the ~ 100 nm size debris particles seen in Figs 11a and b. Specifically, it is suggested that:

1. they come into existence as larger micrometre-scale particles formed by coalescence of cracks which develop wherever primary glide dislocations pile up on intersecting glide planes;
2. because it is constrained by a hydrostatic pressure not too much less than that developed beneath a Vickers diamond indentor, this process operates at a shear stress not too much less than that necessary to form an indentation;
3. in both situations the high shear stress does not imply the occurrence of secondary glide, but rather the need to force primary dislocations to approach to within distances comparable with their core radii in order to overcome the hydrostatic constraint on fracture;
4. when formed initially, the debris particles contain only comparatively few (primary) dislocations, and most of these they quickly lose to the action of image forces;
5. it is comparatively difficult to shear even a micrometre-size particle into two parts through the action of a Frank–Read source;
6. the stress necessary to produce such a shear failure rises and the probability of there being a dislocation available to act as a Frank–Read source falls as particle comminution proceeds and image forces remove more and more dislocations;
7. the stresses required to operate all of these dislocation-controlled processes are large compared to that generated by interaction of the dislocations with irradiation-induced point defects, and hence these processes should be little affected by irradiation;
8. it is unlikely that point contact loading will introduce additional cracks into the debris particles after they form;
9. whatever cracks these particles contain when

they are formed will only propagate in brittle fashion after they become dislocation free;

10. comminution of the debris particles ceased well before they were so far reduced in size that they could no longer store sufficient strain energy to permit further sub-division.

What remains unclear is whether comminution proceeded in its final stages by (brittle) propagation of pre-existing flaws or (ductile) glide of fresh dislocations nucleated at the theoretical shear strength in regions of stress concentration. Regardless of mechanism, however, it appears that comminution stopped because it became easier to accommodate sliding at the contact interface by moving the particles over or past one another as near-rigid (elastic) bodies. Because all three of these processes are expected to be insensitive to irradiation, the insensitivity of the coefficient of friction to this treatment is explained.

Acknowledgements

This work was carried out at The Pennsylvania State University under National Science Foundation Grant no. DMR-8216653. Figs 11a and b were obtained by E. Breval.

References

1. F. P. BOWDEN and D. TABOR, "The Friction and Lubrication of Solids", Vols I and II (Oxford University Press, Oxford, 1954 and 1964).
2. E. MacGURDY, "The Notebooks of Leonardo da Vinci" (Cape, London, 1956).
3. G. AMONTONS, *Mém. Acad. Roy.* **A** (1699) 275.
4. C. A. COULOMB, *Mém. Math. Phys. Acad. Roy.* (1785) 161.
5. J. LESLIE, "An Experimental Enquiry Into the Nature and Propagation of Heat" (Mawman, London, 1804).
6. M. T. SPRACKLING, "The Plastic Deformation of Simple Ionic Crystals" (Academic Press, London, 1976) p. 71.
7. A. KELLY and N. H. MACMILLAN, "Strong Solids", 3rd Edn (Oxford University Press, Oxford, 1986) pp. 116, 143.
8. K. L. KLIEWER and J. S. KOEHLER, *Phys. Rev.* **140** (1965) A1226.
9. *Idem, ibid.* **140** (1965) A1241.
10. R. M. LATANISION and J. T. FOURIE (eds), "Surface Effects in Crystal Plasticity" (Noordhoff, Leyden, The Netherlands, 1977).
11. R. M. LATANISION and J. R. PICKENS (eds), "Atomistics of Fracture" (Plenum Press, New York, 1983).
12. R. M. LATANISION and R. H. JONES (eds), "Chemistry and Physics of Fracture" (Nijhoff, Dordrecht, The Netherlands, 1987).
13. J. H. WESTBROOK and P. J. JORGENSEN, *Trans. Met. Soc. AIME* **233** (1965) 425.
14. R. E. HANNEMAN and J. H. WESTBROOK, *Phil. Mag.* **18** (1968) 73.
15. D. H. BUCKLEY, "Influence of Surface Active Agents on Friction, Deformation and Fracture of Lithium Fluoride", Report NASA TN D-4716 (NASA, Washington, D.C., 1968).
16. Ye. D. SHCHUKIN, V. I. SAVENKO, L. A. KOCHANOVA and P. A. REBINDER, *Dokl. Akad. Nauk. SSSR* **200** (1971) 406.
17. *Idem, ibid.* **200** (1971) 1329.
18. A. A. SHPUNT and O. A. NABUTOVSKAYA, *Sov. Phys. Solid State* **15** (1973) 192.
19. N. H. MACMILLAN, R. D. HUNTINGTON and A. R. C. WESTWOOD, *Phil. Mag.* **28** (1973) 923.
20. A. R. C. WESTWOOD, R. D. HUNTINGTON and N. H. MACMILLAN, *J. Appl. Phys.* **44** (1973) 5194.
21. V. I. SAVENKO, L. A. KOCHANOVA and E. D. SHCHUKIN, *Wear* **56** (1979) 297.
22. F. C. BROWN, University of Washington, Seattle, personal communication (1989).
23. J. GITTUS, "Irradiation Effects in Crystalline Solids" (Applied Science, London, 1978) p. 237.
24. K. GUCKELSBERGER and K. NEUMAIER, *J. Phys. Chem. Solids* **36** (1975) 1353.
25. W. G. JOHNSTON, in "Progress in Ceramic Science", Vol. 2, edited by J. E. Burke (Pergamon Press, New York, 1962) p. 1.
26. K. SANGWAL, "Etching of Crystals" (North-Holland, Amsterdam, The Netherlands, 1987) p. 407.
27. A. ROTH, "Vacuum Technology" (North-Holland, Amsterdam, The Netherlands, 1976).
28. E. A. SCHLANGER, MS thesis, The Pennsylvania State University (1986).
29. C. -Y. HUANG, MS thesis, The Pennsylvania State University (1986).
30. R. C. WEAST (ed.), "Handbook of Chemistry and Physics", 56th Edn (Chemical Rubber Co., Cleveland, 1975/6) p. B-107.
31. J. J. GILMAN, in "The Science of Hardness Testing and Its Research Applications", edited by J. H. Westbrook and H. Conrad (ASM, Metals Park, Ohio, 1973) p. 51.
32. *Idem, J. Appl. Phys.* **44** (1973) 982.
33. *Idem, Acta Metall.* **7** (1959) 608.
34. D. G. RICKERBY, B. N. PRAMILA BAI and N. H. MACMILLAN, in "Energy and Ceramics", edited by P. Vincenzini (Elsevier, Amsterdam, 1980) p. 752.
35. C. A. BROOKES, J. B. O'NEILL and B. A. W. REDFERN, *Proc. Roy. Soc.* **A322** (1971) 73.
36. C. A. BROOKES, R. P. BURNAND and J. E. MORGAN, *J. Mater. Sci.* **10** (1975) 2171.
37. S. G. ROBERTS, *Phil. Mag.* **A58** (1988) 347.
38. S. G. ROBERTS, P. D. WARREN and P. B. HIRSCH, *Mater. Sci. Engng* **A105/106** (1988) 19.
39. Z. G. LIU and W. SKROTZKI, *Phys. Status Solidi (a)* **70** (1982) 433.
40. J. GRUNZWEIG, I. M. LONGMAN and N. J. PETCH, *J. Mech. Phys. Solids* **2** (1954) 81.
41. W. JOHNSON, F. U. MAHTAB and J. B. HADDOW, *Int. J. Mech. Sci.* **6** (1964) 329.
42. L. A. DAVIS and R. B. GORDON, *J. Appl. Phys.* **39** (1968) 3885.
43. P. HAASEN, L. A. DAVIS, E. ALADAG and R. B. GORDON, *Scripta Metall.* **4** (1970) 55.
44. G. FONTAINE and P. HAASEN, *Phys. Status Solidi* **31** (1969) k67.
45. F. A. MOHAMED and T. G. LANGDON, *J. Appl. Phys.* **45** (1974) 1965.
46. P. HAASEN, *Mater. Sci. Technol.* **1** (1985) 1013.
47. A. H. COTTRELL, "Dislocations and Plastic Flow in Crystals" (Oxford University Press, Oxford, 1953) p. 54.
48. R. C. EVANS, "An Introduction to Crystal Chemistry", 2nd Edn (Cambridge University Press, Cambridge, 1964) p. 37.
49. G. SIMMONS and H. WANG, "Single Crystal Elastic Constants and Calculated Aggregate Properties" (MIT Press, Cambridge, 1971) p. 42.
50. J. J. GILMAN and W. G. JOHNSTON, *Solid State Phys.* **13** (1962) 147.
51. R. J. STOKES, *Trans. Met. Soc. AIME* **224** (1962) 1227.
52. K. C. GORETTA and J. L. ROUTBORT, *J. Mater. Sci. Lett.* **6** (1987) 862.
53. A. D. WHAPHAM and M. J. MAKIN, *Phil. Mag.* **5** (1960) 237.
54. N. P. SCVORTZOVA and G. P. BEREZKHOVA, *Cryst. Res. Tech.* **21** (1986) 939.
55. D. M. MARSH, *Phil. Mag.* **5** (1960) 1197.
56. *Idem*, in "Fracture of Solids", edited by D. C. Drucker and J. J. Gilman (Wiley, New York, 1963) p. 119.
57. A. N. STROH, *Adv. Phys.* **6** (1957) 418.
58. P. W. TASKER, *Phil. Mag.* **39** (1979) 119.
59. J. J. GILMAN, *J. Appl. Phys.* **31** (1960) 2208.

60. S. J. BURNS and W. W. WEBB, *ibid.* **41** (1970) 2086.
61. F. C. FRANK and W. T. READ, *Phys. Rev.* **79** (1950) 722.
62. K. KENDALL, *Nature* **272** (1978) 710.
63. *Idem, J. Mater. Sci.* **11** (1976) 1267.
64. *Idem, Proc. Roy. Soc.* **A361** (1978) 245.
65. J. T. HAGAN, *J. Mater. Sci. Lett.* **16** (1981) 2909.
66. D. A. RIGNEY, L. H. CHEN, M. G. S. NAYLOR and A. R. ROSENFIELD, *Wear* **100** (1984) 195.
67. E. BREVAL, J. BREZNAK and N. H. MACMILLAN, *J. Mater. Sci.* **21** (1986) 931.

Received 20 November 1989
and accepted 19 February 1990